

Sodium channel-mediated intrinsic mechanisms underlying the differences of spike programming among GABAergic neurons

Na Chen^a, Yan Zhu^b, Xin Gao^a, Sudong Guan^b, Jin-Hui Wang^{a,b,*}

^a State Key Lab for Brain and Cognitive Sciences, National Lab for Protein Sciences, The Institute of Biophysics, Chinese Academy of Sciences, Beijing 100101, China

^b Department of Physiology, Bengbu Medical College, Anhui 233000, China

Received 16 May 2006

Available online 30 May 2006

Abstract

Neural codes to guide well-organized behavior are thought to be the programmed patterns of sequential spikes at central neurons, in which the coordinative activities of voltage-gated ion channels are involved. The attention has been paid to study the role of potassium channels in spike pattern; but it is not clear how the intrinsic mechanism mediated by voltage-gated sodium channels (VGSC) influences the programming of sequential spikes, which we investigated at GABAergic cerebellar Purkinje cells and hippocampal interneurons by patch-clamp recording in brain slices. Spike capacity is higher at Purkinje cells than interneurons in response to the given intensities of inputs, and is dependent on input intensity. Compared to interneurons, Purkinje cells express the lower threshold potentials and the shorter refractory periods of sequential spikes. The increases of input intensities shorten spike refractory periods significantly. The threshold potentials for VGSC activation and the refractory periods for its reactivation are lower at Purkinje cells, and are reduced by the strong depolarization. We suggest that the VGSC-mediated threshold potentials and refractory periods are regulated by synaptic inputs, and navigate the programming of sequential spikes at the neurons.

© 2006 Elsevier Inc. All rights reserved.

Keywords: Voltage-gated sodium channels; Refractory period; Threshold potential; Action potential; Plasticity; Purkinje cell; Hippocampus

The precise and high-capacity spikes programmed at the neurons constitute the meaningful neural signals that guide the well-organized behaviors in the perception, motion, and cognition under physiological conditions. The programming of sequential spikes, likely the pulse signals produced by a silicon-based switch, is thought of the preferred candidates for the neural computation [1–5]. The spike timing is also critically important [6–8] since precise and loyal spike patterns signify the neuronal events in the meaningful and memorable manner. It is needed to elucidate mechanisms controlling the programming of sequential spikes.

The various types of neurons in the central nervous system fire sequential spikes with the huge diversities [9–15]. In addition to the electrophysiological signature of the

different neurons, such diversified patterns in firing sequential spikes likely constitute the neural codes based on the spike subtypes of neurons in the network to program elegant behaviors. Little is known about the intrinsic mechanisms underlying the precise setting of such diversified patterns among the different neurons [6,16].

The spike patterns are believed to be modulated by synapse dynamics [14,17,18], the membrane potentials [2,19–29], as well as the threshold potentials and refractory periods [6,30]. It is not clear about how the input dynamics drive the firing of sequential spikes, as well as how the interactions between inputs and intrinsic properties mediated by voltage-gated sodium channels (VGSC) navigate sequential spikes. To these questions above, we investigated spike patterns, intrinsic properties, and VGSC kinetics by patch-clamp recordings at GABAergic cerebellar Purkinje cells and hippocampal interneurons in brain slices.

* Corresponding author.

E-mail address: jhw@sun5.ibp.ac.cn (J.-H. Wang).

Materials and methods

Brain slices and neurons studied. Cerebellar and hippocampal slices (400 μm) were prepared from Sprague–Dawley rats in postnatal days (PND 18–20). Rats were anesthetized by injecting pentobarbital (50 mg/kg) and decapitated with a guillotine. Hippocampal and sagittal cerebellar slices were cut with vibratome in the oxygenated (95% O_2 and 5% CO_2) artificial cerebrospinal fluid (ACSF) in the concentration of millimolars (124 NaCl, 3 KCl, 1.2 NaH_2PO_4 , 26 NaHCO_3 , 0.5 CaCl_2 , 4 MgSO_4 , 10 dextrose, and 5 HEPES; pH 7.35) at 4 $^\circ\text{C}$. The slices were held in (95% O_2 and 5% CO_2) ACSF (124 NaCl, 3 KCl, 1.2 NaH_2PO_4 , 26 NaHCO_3 , 2.4 CaCl_2 , 1.3 MgSO_4 , 10 dextrose, and 5 HEPES; pH 7.35) at 25 $^\circ\text{C}$ for 2 h. A slice was transferred to a submersion chamber (Warner RC-26 G) that was perfused with the oxygenated ACSF at 31 $^\circ\text{C}$ for whole-cell recording [15,31]. Chemicals were from Sigma. The procedures were approved by IACUC in Beijing and Anhui China.

Purkinje cells in cerebellar cortex (a round/ovary-like soma and tree branch-like dendrites), as well as multi-polar interneurons in stratum radiatum of hippocampal CA1 area, were recorded by patch-clamp under DIC optics (Nikon FN-600). The recording neurons were labeled by neurobiotin staining after experiments since it was back-filled in the recording pipettes (Fig. 1A; [31] for methods).

Whole-cell recordings. The recordings were conducted in current-clamp model with an Axoclamp-2B amplifier (Axon Instrument Inc., Foster CA, USA); and electrical signals were inputted into pClamp 9 (Axon Instrument, Inc.) for data acquisition and analysis. Output bandwidth in amplifiers was 3 kHz. The spike patterns were evoked by depolarization current pulses, in which the amplitude and duration were based on the aim of experiments. Pipettes for whole-cell recordings were filled with the standard solution that contained (mM) 150 K-gluconate, 5 NaCl, 5 HEPES, 0.4 EGTA, 4 Mg-ATP, 0.5 Tris-GTP, and 5 phosphocreatine (pH 7.35 adjusted by 2 M KOH). Fresh pipette solution was filtered with centrifuge filters (0.1 μm pores) before use and the osmolarity was 295–305 mOsmol. Pipette resistance was 5–6 $\text{M}\Omega$.

The intrinsic properties. Of cerebellar Purkinje cells and hippocampal interneurons in our investigation include the threshold potentials for initiating spikes and refractory periods following each of spikes. The threshold potentials are a start point of the rising phase of spikes [6,32]. The absolute refractory periods (ARP) of sequential spikes are measured by injecting multiple depolarization current pulses (3 ms and 5% above

threshold levels) into the neurons following each of spikes (see Fig. 2). By changing inter-pulse intervals, we define ARP as a duration from a complete spike to a subsequent spike at 50% probability [6]. Spike capacity is represented as inter-spike intervals (ISI).

Single-channel recording. The signals from VGSC were recorded in cell-attached configuration with multi-clamp 700B and pClamp-9 at neurons in cortical slices. Seal resistance was above 20 $\text{G}\Omega$ and pipette resistance was 10–15 $\text{M}\Omega$. Pipette solution contains (mM) 120 NaCl, 2 MgCl_2 , 10 HEPES, 30 TEA, and 0.1 mibefradil. TEA and mibefradil were used to block voltage-gated potassium and type-T calcium channels, respectively. Threshold potentials for VGSC activation were measured when adding negative voltage pulses (4 ms) into the recording pipettes; and refractory periods for VGSC reactivation were measured when changing inter-pulse intervals (IPI) in 4–8 ms. We also measured ARP for VGSC reactivation by raising depolarization intensity. The events of single VGSCs in Fig. 4 are summated.

Data were analyzed if the recorded neurons had the resting membrane potentials negatively more than -55 mV. The criteria for the acceptance of each experiment also included less than 5% changes in resting membrane potential, spike magnitude, input resistance, and seal resistance throughout each of experiments. Input resistance was monitored by measuring cell responses to the hyperpolarization pulses at the same values as the depolarization that evoked spikes. Vts, ARP, and ISI are presented as means \pm SE. The comparisons between groups are done by *t* test.

Results

VGSC-mediated intrinsic mechanisms underlying spike programming are studied with whole-cell and cell-attached single channel recordings at GABAergic cerebellar Purkinje cells and hippocampal interneurons in brain slices.

Spike capacity is higher at Purkinje cells than hippocampal interneurons

Purkinje cells (PC) and hippocampal interneurons (IN) are recorded by whole-cell current clamp, and identified

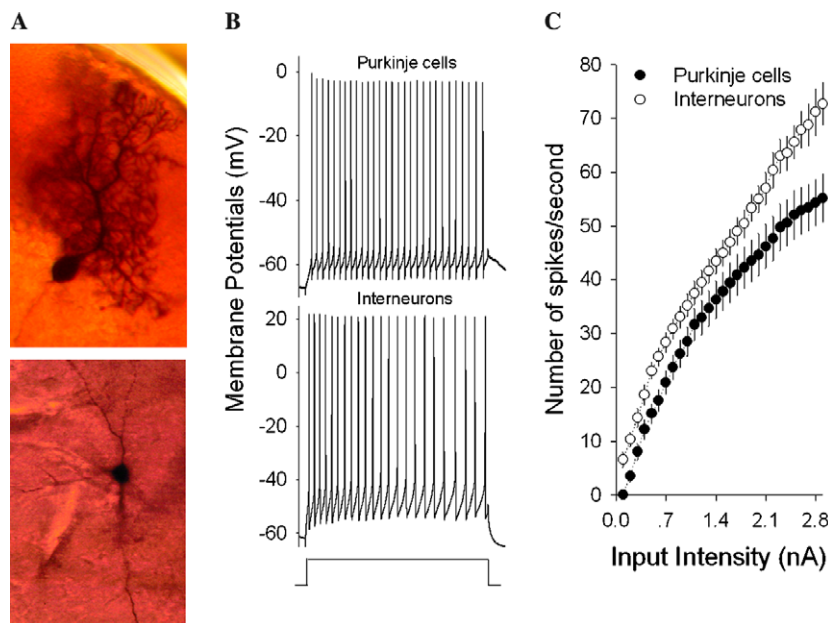


Fig. 1. The firing patterns of sequential spikes at the cerebellar Purkinje cells and hippocampal interneurons. (A) The neurons are labeled by neurobiotin, in which the pipettes are used to record neuronal signals and inject neurobiotin, Purkinje cells (top panel), and interneurons (bottom panel). (B) Spikes are evoked by injecting the current pulses (1 s) with the same intensity at Purkinje cells (top panel) and interneurons (bottom). (C) The comparisons of spike capacity vs. input intensities between Purkinje cells ($n = 14$) and interneurons, where spike capacity is higher at Purkinje cells ($n = 32$, $p < 0.01$).

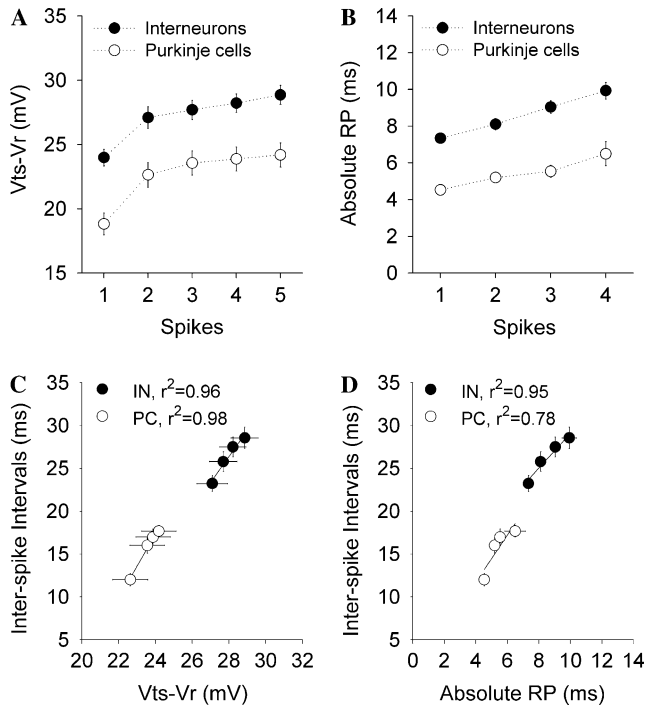


Fig. 2. The intrinsic properties of sequential spikes are different between cerebellar Purkinje cells and hippocampal interneurons. (A) The comparison of threshold potentials ($V_{ts}-V_r$) of spike 1–5 between Purkinje cells ($n = 30$, opened symbols) and interneurons ($n = 32$, filled symbols). (B) The comparison of absolute refractory periods (ARP) of spike 1–4 between Purkinje cells ($n = 30$, opened symbols) and interneurons ($n = 32$, filled symbols). (C) The linear correlations between $V_{ts}-V_r$ and inter-spike intervals at Purkinje cells ($r^2 = 0.98$, opened symbols) and interneurons (fast-spiking neurons, FSN, $r^2 = 0.96$, filled symbols). (D) The linear correlations between ARP and inter-spike intervals at Purkinje cells ($r^2 = 0.78$, opened symbols) and interneurons (fast-spiking neurons, FSN, $r^2 = 0.95$, filled symbols).

by neurobiotin-labeling (top panel for PC and bottom for IN, respectively, in Fig. 1A). Sequential spikes were evoked by injecting the different strengths of current pulses (1 s) into these neurons. Spike patterns appear tonic at PC (top panel in Fig. 1B) and IN (bottom panel). Fig. 1C illustrates the averaged data of the intensities of current pulses (nA) vs. spike capacity (the number of spikes per second) at Purkinje cells (opened symbols, $n = 14$) and interneurons (filled symbols, $n = 32$). To the given intensities, the spike capacity at Purkinje cells and interneurons is statistically different ($p < 0.01$). These results indicate that spike capacity at the central neurons is proportional to the input intensity, and that Purkinje cells have a high ability to program sequential spikes in response to synaptic inputs.

The mechanisms underlying the indications above are hypothetically the neuronal intrinsic properties, which are granted by the following facts. Spike patterns are linearly correlated with threshold potentials and refractory periods [6]. The difference of spike capacity between these two kinds of neurons is resulted from their intrinsic properties since current pulses to evoke their spikes are given in the same intensities (Fig. 1C). The input intensity-dependent change in spike capacity (Fig. 1C) implies the plasticity

of membrane intrinsic property driven by the strength of synaptic inputs. We tested these hypotheses below.

Threshold potentials and refractory periods of spikes are lower at Purkinje cells

To the fact that the spike capacity is higher at Purkinje cells than interneurons, we assumed that the refractory periods of sequential spikes are shorter at Purkinje cells, which allow subsequent spikes to move toward their front ones, as well as that the threshold potentials are lower at Purkinje cells, which widens the band of firing spikes. With measuring such two parameters [6], we compared intrinsic properties underlying the different spike capacity at cerebellar Purkinje cells and hippocampal interneurons.

Fig. 2A illustrates the comparisons of threshold potentials ($V_{ts}-V_r$) for sequential spikes between Purkinje cells and interneurons. The values of $V_{ts}-V_r$ from spikes 1–5 are 18.82 ± 0.85 , 22.64 ± 0.96 , 23.56 ± 0.94 , 23.87 ± 0.94 , and 24.19 ± 0.94 mV at Purkinje cells (opened circles, $n = 21$); and the values are 23.98 ± 0.65 , 27.1 ± 0.84 , 27.69 ± 0.75 , 28.22 ± 0.71 , and 28.86 ± 0.73 mV at interneurons (filled circles, $n = 32$). $V_{ts}-V_r$ values relevant to the same number in sequential spikes in these two kinds of neurons are statistically different ($p < 0.01$).

Fig. 2B demonstrates the comparisons of absolute refractory periods (ARP) for sequential spikes between Purkinje cells and interneurons. ARP values for spikes 1–4 are 4.53 ± 0.2 , 5.19 ± 0.27 , 5.53 ± 0.3 , and 6.49 ± 0.67 ms at Purkinje cells (opened circles, $n = 16$); and values for ARP_{1–4} are 7.33 ± 0.27 , 8.11 ± 0.31 , 9.1 ± 0.35 , and 9.93 ± 0.46 ms at interneurons (filled circles, $n = 32$). ARP values relevant to the same number in sequential spikes at these two kinds of neurons are statistically different ($p < 0.01$).

These results are consistent with our prediction that the threshold potentials are lower and refractory periods are shorter at cerebellar Purkinje cells than interneurons. Moreover, the threshold potentials are linearly correlated with inter-spike intervals at Purkinje cells (opened symbols in Fig. 2C) and interneurons (filled symbols in Fig. 2C); and the refractory periods are linearly correlated with inter-spike intervals at Purkinje cells (opened symbols in Fig. 2D) and interneurons (filled symbols in Fig. 2D). Together with the results above, we conclude that the shorter refractory periods and lower threshold potentials result in the higher capacity of spike programming at Purkinje cells.

The plasticity of refractory periods is driven by input intensities

In terms of the mechanism underlying a fact that spike capacity is increasing with input intensities (Fig. 1C), we hypothesized that neuronal intrinsic properties (such as refractory periods) undergo a dynamic plasticity when input intensity is changing. For instance, an increase in input inten-

sity shortens refractory periods and in turn reduces interspike intervals, which allow spike capacity being increased.

We tested this hypothesis by measuring the absolute refractory periods (ARP) of sequential spikes [6] under injecting different strengths of current pulses at Purkinje cells (Fig. 3A and B) and hippocampal interneurons (Fig. 3C and D). Fig. 3A illustrates the measurement of ARP subsequent to spike one and three under weaker stimuli (blue traces) and stronger stimuli (reds) at Purkinje cells. For the comparisons among neurons, stimulus intensities were normalized based on threshold stimuli that were current pulses (3 ms) to evoke a single spike and defined as one. Fig. 3B shows the plot of the normalized threshold stimuli (Tsti.) vs. ARP for spike-1 (open symbols) and spike-3 (filled symbols). These two parameters are inversely correlated in a linear manner ($r_1^2 = 0.97$ for spike-1 and $r_3^2 = 0.94$ for spike-3) at Purkinje cells. Similarly, Fig. 3C shows the measurement of ARP subsequent to spike one and three under weaker stimuli (blue traces) and stronger stimuli (reds) at hippocampal interneurons. Fig. 3D shows the plot of the normalized Tsti vs. ARP for spike-1 (open symbols) and spike-3 (filled symbols). Two parameters are inversely correlated in a linear manner ($r_1^2 = 0.99$ for spike-1 and $r_3^2 = 0.91$ for spike-3) at interneurons.

A fact that the stronger inputs are associated with the shorter ARP at these two kinds of neurons grants that input-dependent increase in spike capacity is resulted from the reduction of refractory periods, and moreover, the plasticity of synaptic inputs may cause the dynamic plasticity of neuronal spike programming. It is noteworthy that the values of linear slope for spike-3 are -3.65 at cerebellar Purkinje cells, and -7.5 at hippocampal interneurons, implying that the dynamics of input-driven plasticity in the refractory periods mediated by voltage-gated sodium channels are different between these two kinds of neurons. In addition, absolute value for the linear slope of spike-3 (-7.5) is larger than that for spike-1 (-3.4) at hippocampal interneurons, i.e., the higher intensity of inputs more efficiently reduces ARP in the late phase of sequential spikes, implying that synaptic potentiation mainly improves spike programming in late phase.

The plasticity of VGSC kinetics underlies the variations of spike capacity

The threshold potentials and refractory periods are lower at Purkinje cells, leading to their higher spike capacity (Figs. 1 and 2). The plasticity of refractory periods driven

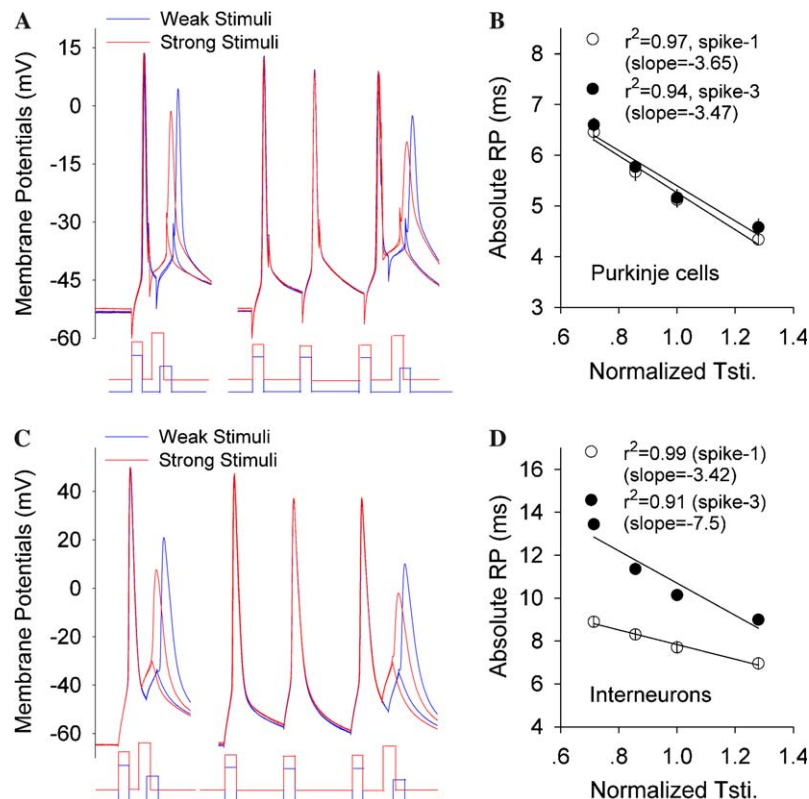


Fig. 3. The inverse linear correlations between absolute refractory periods (ARP) and input intensities at cerebellar Purkinje cells and hippocampal interneurons. (A) The measurement of the influence of input strength on the ARP of sequential spikes, e.g., spike-1 (left) and spike-3 (right), at cerebellar Purkinje cells (blue traces for weak-input and red traces for strong-input strength). (B) The linear correlation between the normalized stimuli and ARP for spike-1 (linear slope, -3.65) and spike-3 (linear slope, -3.47). (C) The measurement of the influence of input strength on the ARP of sequential spikes, e.g., spike-1 (left) and spike-3 (right), at hippocampal interneurons (blue traces for weak-input and red traces for strong-input strength). (D) The linear correlation between the normalized stimuli and ARP for spike-1 (linear slope, -3.42) and spike-3 (slope, -7.5). (For interpretation of the references to color in this figure legend, the reader is referred to the web version of this paper.)

by input intensity allows the proportional increase of spike capacity with input intensities (Figs. 1 and 3). If voltage-gated sodium channels (VGSC) mechanistically influence V_t and ARP, the thresholds for VGSC activation and refractory periods for its reactivation should be lower at Purkinje cells; and VGSC activities be higher when the membrane depolarization is increased. We examined these predictions below.

With cell-attached configuration, we recorded the currents of single VGSCs and depolarized the potentials of patch membrane by applying depolarization pulses (DP, 15–40 mV and 4 ms) to find the thresholds for VGSC activation and activity levels. The inter-pulse intervals (IPI) of sequential pulses are various in 4–8 ms to search for the refractory periods for VGSC reactivation. Fig. 4 shows VGSC activities from one of examples ($n = 10$) at cerebellar Purkinje cells (A–D) and hippocampal interneurons (E–H) under the different values of membrane depolarization and inter-pulse intervals.

In cerebellar Purkinje cells, the threshold potentials for VGSC activation are read in a range of DP 15–20 mV (Fig. 4A and B). The refractory periods for VGSC reactivation after pulse one are between 4 and 6 ms (Fig. 4B and C). These values are similar to those of spike thresholds and refractory periods in Fig. 2. When we applied DP 35 mV and IPI 4 ms, VGSC can be activated by five sequential pulses (Fig. 4D). Compared to Fig. 4B, this result indicates that the increases in input intensities shorten the refractory periods for VGSC reactivation, similar to a fact that the refractory periods for spikes are shortened by increasing input intensities (Fig. 3A and B). Such changes in the dynamics of VGSC grant our prediction that the thresholds and refractory periods of sequential spikes are governed by VGSC properties.

In hippocampal interneuron, the threshold potentials for VGSC activation are read in DP 25–30 mV (Fig. 4E and F). The refractory periods for VGSC reactivation after pulse one are between 6 and 8 ms (Fig. 4F and G).

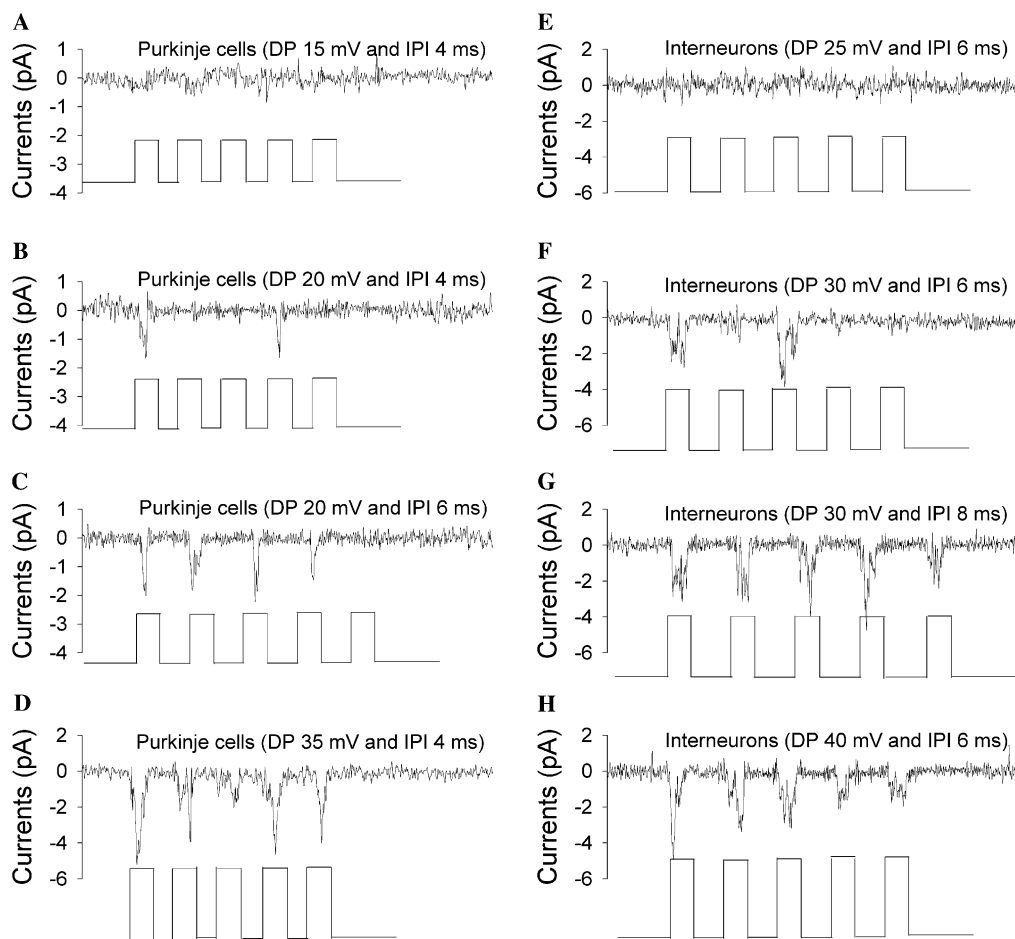


Fig. 4. The threshold potentials, refractory periods, and voltage-dependent activity of voltage-gated sodium channels (VGSC) are different on the membrane between cerebellar Purkinje cells and hippocampal interneurons. (A–D) An example of VGSC recordings from Purkinje cells; and (E–H) an example from interneuron. (A) VGSC is not activated by depolarization pulses (DP, 15 mV and 4 ms) and inter-pulse intervals (IPI) 4 ms. (B) VGSC is activated by DP 20 mV, but barely activated by subsequent pulses with IPI 4 ms. (C) VGSC is activated by DP 20 mV and subsequent pulses with IPI 6 ms. (D) VGSC is more active by DP 35 mV and subsequent pulses with IPI 4 ms. (E) VGSC is not activated by DP 25 mV (4 ms) and inter-pulse intervals (IPI) 6 ms. (F) VGSC is activated by DP 30 mV, but barely activated by subsequent pulses with IPI 6 ms. (G) VGSC is activated by DP 30 mV and subsequent pulses with IPI 8 ms. (H) VGSC is more active by DP 40 mV and subsequent pulses with IPI 6 ms.

These values are similar to those of spike thresholds and refractory periods in Fig. 2. When we applied DP 40 mV and IPI 6 ms, VGSC can be activated by five sequential pulses (Fig. 4H). Compared to Fig. 4F, this result indicates that an increase in input intensities reduces the refractory periods for VGSC reactivation, consistent with a fact that refractory periods for spikes are shortened by increasing input intensities (Fig. 3C and D). The results are similar to those at Purkinje cells.

It is noteworthy that threshold potentials for VGSC activation are lower at Purkinje cells (Fig. 4A, B and E, F), and that the refractory periods for VGSC reactivation are shorter at Purkinje cells (Fig. 4B, C and F, G). Moreover, when membrane depolarization is increased, the currents of VGSC are increasingly larger, indicating either the more opening of single VGSC or the activation of more channels in this membrane patch.

Discussion

Our results demonstrate that spike capacity is higher at cerebellar Purkinje cells than hippocampal interneurons and that the number of spikes increases proportionally to input intensities. With measuring the threshold potentials and refractory periods of sequential spikes as well as voltage-gated sodium channel dynamics, we found that the threshold potentials to initiate spikes are lower and the refractory periods to evoke subsequent spikes are shorter at Purkinje cells than interneurons. The capacity of sequential spikes is linearly correlated with their threshold potentials and refractory periods; and the refractory periods are shortened by raising input intensities at both neurons. The threshold potentials for VGSC activation and refractory periods for its reactivation are lower at Purkinje cells. An increase in the membrane depolarization reduces the refractory periods for VGSC reactivation and evokes VGSC being more active at both kinds of neurons. Our findings can well explain the variations of spike capacity among different neurons as well as under the different intensities of inputs.

The number of spikes evoked by the given inputs is higher at cerebellar Purkinje cells than hippocampal interneurons. If spikes represent the digital “1”, and inter-spike intervals are “0” in the computation of neural signals [30], Purkinje cells have high ability in signal encoding to execute their inhibitory function compared to hippocampal interneurons. In terms of its mechanisms, the threshold potentials and refractory periods influence the capacity of sequential spikes, since they are linearly correlated. The lower threshold potentials at Purkinje cells make them more sensitive to the given synaptic inputs. The shorter refractory periods make subsequent spikes shift toward initial ones, increasing the number of spikes in a given period. Moreover, the threshold potentials for VGSC activation and refractory periods for its reactivation are lower at Purkinje cells, which grant the lower thresholds and shorter refractory periods of sequential spikes for higher spike

capacity. It remains to be studied if these intrinsic mechanisms vary among other neurons to control their spike capacity.

The number of spikes increases proportionally to input intensities at cerebellar Purkinje cells and hippocampal interneurons, i.e., spike capacity (the ability of spike programming) is influenced by the strength of synaptic inputs, in addition to neuronal intrinsic properties. In other words, synaptic plasticity may influence the programming of neuronal signals to change the inhibitory function of these neurons. We found that the refractory periods of sequential spikes are reduced by increasing input intensities, and that refractory periods for VGSC reactivation are shortened by raising membrane depolarization. These results indicate that the refractory periods mediated by VGSC undergo the plasticity, which is driven by the plasticity of synaptic strength. In addition to this plasticity of refractory periods underlying input-dependence of spike capacity, more activities of VGSCs by a strong depolarization may be involved. It is being studied whether more VGSCs are activated by the stronger depolarization, i.e., there are the subgroups of VGSCs in their activation thresholds, on a single neuron or the voltage-dependent changes in the conductance of a single VGSC are present.

The threshold potentials for VGSC activation and the refractory periods for VGSC reactivation are different at cerebellar Purkinje cells and hippocampal interneurons (Fig. 4). The mechanism underlying the variations of VGSC dynamics among neurons remains to be studied. VGSC is regulated by intracellular signal molecules, such as protein kinase C [33] and calmodulin-dependent protein kinases [34]. If the activities of these signal molecules vary among the neurons, the kinetics of VGSCs on those cells should be different. On the other hand, VGSCs are classified into several subtypes based on genetic studies [35,36] or on functional properties [37]. This grants a possibility that the different subtypes of VGSCs are located at Purkinje cells and interneurons (our unpublished data) for their expression of various intrinsic properties to guide spike programming.

In terms of the mechanisms underlying the phenomenon that the enhanced input strengths shorten the refractory periods for VGSC reactivation and increase its activity (Fig. 4), we suggest that the voltage pulses influence VGSC kinetics directly since the depolarization of the patch membrane is not sufficient to evoke spikes. Without an activation of intracellular signal cascades by spike-related Ca^{2+} increase, the plasticity of VGSC kinetics should be simply resulted from altering the membrane potentials, i.e., voltage-dependent in nature. This short-term plasticity in the intrinsic properties is different from a long-term change that is intracellular Ca^{2+} -dependent [32]. It is pointed out that with measuring the refractory periods and threshold potentials of sequential spikes and VGSC kinetics, our data grant an assumption that VGSCs underlie the threshold potentials and refractory periods in the genetic studies [33,38–40].

We discovered that VGSC-mediated intrinsic properties (threshold potentials and refractory periods) govern the programming of sequential spikes at central neurons beyond a role of potassium channels [20–23,25,26]. Our data provide clues for elucidating cellular and molecular mechanisms underlying the precise analysis and computation of neural signals that are neural language to guide well-organized behaviors.

Acknowledgment

This study is designed and written by J.-H.W. and is supported by National Awards for the Outstanding Young Scientist (30325021), Natural Science Foundation China (NSFC30470362), NSFC (30621130077), and National Basic Research Program 2006CB500804 to J.-H.W.

References

- [1] C. Koch, Computation and the single neuron, *Nature* 385 (1997) 207–210.
- [2] M. London, A. Schreibleman, M. Hausser, M.E. Larkum, I. Segev, The information efficacy of a synapse, *Nat. Neurosci.* 5 (2002) 332–340.
- [3] M.N. Shadlen, W.T. Newsome, Noise, neural codes and cortical organization, *Curr. Opin. Neurobiol.* 4 (1994) 569–579.
- [4] N.C. Spitzer, P.A. Kingston, T.J. Manning Jr., M.W. Conklin, Outside and in: development of neuronal excitability, *Curr. Opin. Neurobiol.* 12 (2002) 315–323.
- [5] P.H.E. Tiesinga, J.V. Toups, The possible role of spike patterns in cortical information processing, *J. Comput. Neurosci.* 18 (2005) 275–286.
- [6] N. Chen, S.L. Chen, Y.L. Wu, J.-H. Wang, The measurement of threshold potentials and refractory periods of sequential spikes by whole-cell recordings, *Biochem. Biophys. Res. Commun.* 340 (2006) 151–157.
- [7] D. Fricker, R. Miles, Interneuron, spike timing, and perception, *Neuron* 32 (2001) 771–774.
- [8] R.S. Petersen, S. Panzeri, M.E. Diamond, Population coding in somatosensory cortex, *Curr. Opin. Neurobiol.* 12 (2002) 441–447.
- [9] A. Destexhe, M. Rudolph, D. Pare, The high-conductance state of neocortical neurons in vivo, *Nat. Rev. Neurosci.* 4 (2003) 739–751.
- [10] T.F. Freund, G. Buzsáki, Interneurons of the hippocampus, *Hippocampus* 6 (1996) 347–470.
- [11] J.A. Hobson, E.F. Pace-Schott, The cognitive neuroscience of sleep: neuronal system, consciousness and learning, *Nat. Rev. Neurosci.* 3 (2002) 679–693.
- [12] H. Markram et al., Interneurons of the neocortical inhibitory system, *Nat. Rev. Neurosci.* 5 (2004) 793–807.
- [13] C.J. McBain, A. Fisahn, Interneurons unbound, *Nat. Rev. Neurosci.* 2 (2001) 11–23.
- [14] P. Somogyi, T. Klausberger, Defined types of cortical interneuron structure space and spike timing in the hippocampus, *J. Physiol. (London)* 562 (2005) 9–29.
- [15] J.-H. Wang, Short-term cerebral ischemia causes the dysfunction of interneurons and more excitation of pyramidal neurons, *Brain Res. Bull.* 60 (2003) 53–58.
- [16] S. Grillner, H. Markram, E.D. Schutter, G. Silberger, F.E.N. LeBeau, Microcircuits in action—from CPGs to neocortex, *Trends Neurosci.* 28 (2005) 525–533.
- [17] D. Daoudal, D. Debanne, Long-term plasticity of intrinsic excitability: learning rules and mechanisms, *Learning Memory* 10 (2003) 456–465.
- [18] W. Zhang, D. Linden, The other side of the engram: experience-driven changes in neuronal intrinsic excitability, *Nat. Rev. Neurosci.* 4 (2003) 885–900.
- [19] J.-M. Fellous, P. Tiesinga, P.J. Thomas, T.J. Sejnowski, Discovering spike patterns in neuronal responses, *J. Neurosci.* 24 (2004) 2989–3001.
- [20] P.A. Glazebrook et al., Potassium channels Kv1.1, Kv1.2 and Kv1.6 influence excitation of rat visceral sensory neurons, *J. Physiol. (London)* 541 (2002) 467–482.
- [21] D. Hess, A.E. Manira, Characterization of a high-voltage-activated I_a current with a role in spike timing and locomotor pattern generation, *Proc. Natl. Acad. Sci. USA* 98 (2001) 5276–5281.
- [22] D. Johnston et al., Dendritic potassium channels in hippocampal pyramidal neurons, *J. Physiol. (London)* 525 (2000) 75–81.
- [23] S. Nedergarrd, Regulation of action potential size and excitability in substantia nigra compacta neurons: sensitivity to 4-aminopyridine, *J. Neurophysiol.* 82 (1999) 2903–2913.
- [24] L.G. Nowak, M.V. Sanchez-Vives, D.A. McCormick, Influence of low and high frequency inputs on spike timing in visual cortical neurons, *Cerebral Cortex* 7 (1997) 487–501.
- [25] B. Rudy et al., Contributions of Kv3 channels to neuronal excitability, *Ann. NY Acad. Sci.* 868 (1999) 304–343.
- [26] P. Sah, Ca^{2+} -activated K^+ currents in neurones: types, physiological roles and modulation, *Trends Neurosci.* 19 (1996) 150–154.
- [27] S. Schreiber, J.-M. Fellous, P. Tiesinga, T.J. Sejnowski, Influence of ionic conductances on spike timing reliability of cortical neurons for suprathreshold rhythmic inputs, *J. Neurophysiol.* 91 (2004) 194–205.
- [28] A. Szucs, A. Vehovszky, G. Molnar, R.D. Pinto, H.D.I. Abarbanel, Reliability and precision of neural spike timing: simulation of spectrally broadband synaptic inputs, *Neuroscience* 126 (2004) 1063–1073.
- [29] M. Wehr, A.M. Zador, Balanced inhibition underlies tuning and sharpens spike timing in auditory cortex, *Nature* 426 (2003) 442–446.
- [30] S. Guan et al., The intrinsic mechanisms underlying the maturation of programming sequential spikes at cerebellar Purkinje cells, *Biochem. Biophys. Res. Commun.* 345 (2006) 175–180.
- [31] J.-H. Wang, P.T. Kelly, Ca^{2+} /CaM signalling pathway up-regulates glutamatergic synaptic function in non-pyramidal fast-spiking neurons of hippocampal CA1, *J. Physiol. (London)* 533 (2001) 407–422.
- [32] M. Zhang, F. Hung, Y. Zhu, Z. Xie, J. Wang, Calcium signal-dependent plasticity of neuronal excitability developed postnatally, *J. Neurobiol.* 61 (2004) 277–287.
- [33] A.R. Catterall, W.A. Catterall, Neuromodulation of Na^+ channels: an unexpected form of cellular plasticity, *Nat. Rev. Neurosci.* 2 (2001) 397–407.
- [34] S. Gasparini, J.C. Magee, Phosphorylation – dependent differences in the activation properties of distal and proximal dendritic Na^+ channels in rat CA₁ hippocampal neurons, *J. Physiol. (London)* (2002) 665–672.
- [35] W.A. Catterall, From ionic currents to molecular mechanisms: the structure and function of voltage-gated sodium channels, *Neuron* 26 (2000) 13–25.
- [36] S.D. Novakovic, R.M. Eglén, J.C. Hunter, Regulation of Na^+ channel distribution in the nervous system, *Trends Neurosci.* 24 (2001) 473–478.
- [37] B.V. Safronov, M. Wolff, W. Vogel, Functional distribution of three types of Na^+ channel on soma and processes of dorsal horn neurons of rat spinal cord, *J. Physiol. (London)* 503 (1997) 371–385.
- [38] R. Azous, C.M. Gray, Dynamic spike threshold reveals a mechanism for synaptic coincidence detection in cortical neurons in vivo, *Proc. Natl. Acad. Sci. USA* 97 (2000) 8110–8115.
- [39] C.M. Colbert, E. Pan, Ion channel properties underlying axonal action potential initiation in pyramidal neurons, *Nat. Neurosci.* 5 (2002) 533–538.
- [40] M.C. Kiernan, A.V. Kirshnan, C.S. Lin, D. Burkke, S.F. Berkovic, Mutation in the Na^+ channel subunit SCN1B produces paradoxical changes in peripheral nerve excitability, *Brain* 128 (2005) 1841–1846.